

# Predictions of $\alpha$ -decay half-lives for neutron-deficient nuclei with the aid of artificial neural network

A. A. SAEED, W. A. YAHYA<sup>†</sup>, O. K. AZEEZ

<sup>†</sup>Department of Physics and Materials Science, Kwara State University, Malete, Nigeria

In recent years, artificial neural network (ANN) has been successfully applied in nuclear physics and some other areas of physics. This study begins with the calculations of  $\alpha$ -decay half-lives for some neutron-deficient nuclei using Coulomb and proximity potential model (CPPM), temperature dependent Coulomb and proximity potential model (CPPMT), Royer empirical formula, new Ren B (NRB) formula, and a trained artificial neural network model ( $T^{ANN}$ ). By comparison with experimental values, the ANN model is found to give very good descriptions of the half-lives of the neutron-deficient nuclei. Moreover CPPMT is found to perform better than CPPM, indicating the importance of employing temperature-dependent nuclear potential. Furthermore, to predict the  $\alpha$ -decay half-lives of unmeasured neutron-deficient nuclei, another ANN algorithm is trained to predict the  $Q_\alpha$  values. The results of the  $Q_\alpha$  predictions are compared with the Weizsäcker-Skyrme-4+RBF (WS4+RBF) formula. The half-lives of unmeasured neutron-deficient nuclei are then predicted using CPPM, CPPMT, Royer, NRB, and  $T^{ANN}$ , with  $Q_\alpha$  values predicted by ANN as inputs. This study concludes that half-lives of  $\alpha$ -decay from neutron-deficient nuclei can successfully be predicted using ANN, and this can contribute to the determination of nuclei at the driplines.

PACS numbers: 27.90.+b; 23.60.+e ; 21.10.Tg ; 23.70.+j

## 1. Introduction

$\alpha$ -decay is one of the most important types of radioactive decay in the study of nuclei [1], owing to its ability to provide insights on nuclear structure and stability of nuclei [2]. It was discovered by Ernest Rutherford in 1899 as a component out of three components of radiation emitted by uranium nucleus [3]. In 1928, Gamow [4], Gurney and Condon [5, 6] gave

---

<sup>†</sup> email: wasiu.yahya@gmail.com

a theoretical explanation of the Geiger-Nuttall law, which derives its basis from the quantum tunneling effect and was the first successful attempt at the quantum description of nuclear phenomena. Since then, many theoretical models and empirical formulas have been proposed to calculate  $\alpha$ -decay half-lives of nuclei. Some of the theoretical models include the effective liquid drop model (ELDM) [7, 8], the generalized liquid drop model (GLDM) [9–11], modified generalized liquid drop model (MGLM) [12, 13], preformed cluster model (PCM) [14, 15], fission-like model [16], and so on. Some of the theoretical models use phenomenological potentials while others use microscopic potentials [17, 18]. Some of the empirical formulas that have been successful in the investigation of  $\alpha$ -decay half-lives are the Royer formula [19–21], Denisov and Khudenko formula [22], Viola and Seaborg formula (VSS) [23], Ren formulas [24] (and the modified Ren formulas [25]), universal decay law (UDL) [26], Akrawy and Poenaru formula [27], etc.

$\alpha$ -decay is a dominant radioactive decay mode for unstable nuclei, particularly neutron-deficient nuclei. An atomic nucleus is said to be neutron-deficient if it consists of more protons than neutrons; they are also called proton-rich nuclei, and are close to the proton drip-line. Most of the observed neutron-deficient nuclei with mass number  $A \geq 150$  can undergo  $\alpha$ -decay. The study of the half-lives of neutron-deficient nuclei can contribute to the determination of nuclei at the driplines. The contribution to the determination of nuclei at the driplines have motivated some researches on nuclei with  $Z > N$  [28–32]. This study will calculate the  $\alpha$ -decay half-lives of neutron-deficient nuclei using Coulomb and proximity potential model and two empirical formulas. It is known that the Coulomb and proximity potential model (CPPM), and temperature dependent Coulomb and proximity potential model (CPPMT) are successful models in the investigation of  $\alpha$ -decay half-lives [33–36]. The two empirical formulas to be employed are the Royer formula [19, 20] and new Ren B formula [25]. These formulas have been known to be successful in the calculation of  $\alpha$ -decay half-lives of nuclei.

In recent years, machine learning has grown in popularity in the physics community due to its ability to learn from data and arrive at reasonable conclusions. The two commonly used techniques in machine learning are supervised and unsupervised learning techniques. In supervised learning, data with labels are used to train the model with the goal of predicting outcomes as accurately as possible. In unsupervised learning, data with no labels are fed into the model with the goal of finding hidden patterns in the data and arriving at reasonable conclusions. Artificial neural network (ANN), which is an algorithm under supervised machine learning contains a large system that is created and programmed to mimic the human brain [37],

and operates by using dense layers made up of neurons to process information. These neurons are also known as units and are arranged in series. The data go through the input layer of the ANN from external sources for the system to learn from and this information is processed in the hidden layer connected by weights, which then becomes the outcome in the output layer. There have been some successful applications of machine learning in nuclear physics. For example machine learning and deep learning have been employed in the study of nuclear charge radii [38, 39], in the predictions of nuclear  $\beta$ -decay half-lives [40], in the extraction of electron scattering cross-sections from swarm data [41], in the shell model calculations for proton-rich zinc (Zn) isotopes [42], and in the prediction of  $\alpha$ -decay  $Q_\alpha$  values [43].

In this paper, we employ the use of the Coulomb and proximity potential model (CPPM) in the calculation of the  $\alpha$ -decay half-lives of some measured neutron-deficient nuclei. Since it is known that the use of temperature-dependent potential can improve the prediction of  $\alpha$ -decay half-lives, we have also used the temperature-dependent Coulomb and proximity potential model (termed CPPMT). Moreover, an artificial neural network (specifically, a multilayer feed forward neural network) is also used to predict the half-lives. Two empirical formulas viz. Royer and new Ren B formulas have also been used to determine the performance accuracy of the CPPM, CPPMT, and ANN models. Since the NUBASE2020 [44, 45] database is now publicly available, the data used in the study have been extracted from the database. New coefficients for the two empirical formulas are determined using a least square fit scheme with input data from the NUBASE2020 database. The study also predicts the half-lives of  $\alpha$ -decay from some unmeasured neutron-deficient nuclei. To achieve this, one requires the  $Q_\alpha$  values for the  $\alpha$ -decay processes. Since there are no experimental  $Q_\alpha$  values for the unmeasured neutron-deficient nuclei, an artificial neural network (ANN) has been trained to predict  $Q_\alpha$  values using about 1021  $Q_\alpha$  values from the NUBASE2020 database. The trained ANN model was then used to predict the  $Q_\alpha$  values for unmeasured neutron-deficient nuclei. The results obtained are compared to the theoretical WS4 and WS4+RBF [46]  $Q_\alpha$  values. The predicted  $Q_\alpha$  values are then used as inputs to predict the  $\alpha$ -decay half-lives of unmeasured neutron-deficient nuclei.

The paper is presented as follows: the theoretical models used are introduced in Section 2. In Section 3, the results of the calculations are presented and discussed, and in Section 4, the conclusion is presented.

## 2. Theoretical Formalism

### 2.1. Coulomb and proximity potential model (CPPM)

In this model, the total interaction potential between the  $\alpha$  particle and the daughter nucleus can be expressed as the summation of the proximity potential, Coulomb potential, and centrifugal potential for both the touching configuration and separated fragments. That is [33]:

$$V = V_C(r) + V_P(z) + \frac{\hbar\ell(\ell+1)}{2\mu r^2}, \quad (1)$$

where the last term is the centrifugal potential,  $\ell$  is the angular momentum carried by the  $\alpha$  particle, the Coulomb potential  $V_C$  given by:

$$V_C(r) = Z_1 Z_2 e^2 \begin{cases} \frac{1}{r} & \text{for } r \geq R_C \\ \frac{1}{2R_C} \left[ 3 - \left( \frac{r}{R_C} \right)^2 \right] & \text{for } r \leq R_C \end{cases}. \quad (2)$$

Here,  $Z_1$  and  $Z_2$  represent the charge number of the  $\alpha$  particle emitted and the daughter nucleus, respectively, and  $r$  is the distance between the fragments centres.  $R_C$  is known as the radial distance and is given by  $R_C = 1.24(R_1 + R_2)$ , where  $R_1$  and  $R_2$  are defined below.

The first recorded implementation of the proximity potential was in 1987 by Shi and Swiatecki where nuclear deformation influence, and the shell effects on the half-life of exotic radioactivity were estimated [47]. Two years later, Malik et al. applied the proximity potential model in the preformed cluster model [48]. The calculation of the strength of the interaction of the daughter and emitted  $\alpha$  particle yields the proximity potential  $V_P(z)$  provided by Blocki et al [49], and is given as:

$$V_P(z) = 4\pi\gamma b\bar{R}\phi\left(\frac{z}{b}\right) \text{ MeV}, \quad (3)$$

where the nuclear surface potential  $\gamma$  is given as

$$\gamma = 1.460734 \left[ 1 - 4 \left( \frac{N - Z}{N + Z} \right)^2 \right] \text{ MeV/fm}^2. \quad (4)$$

Here  $N$  and  $Z$  denote the neutron number and proton number of the parent nucleus, respectively.  $\phi$  is the universal proximity potential, given by [50]:

$$\phi(\epsilon) = \begin{cases} \frac{1}{2}(\epsilon - 2.54)^2 - 0.0852(\epsilon - 2.54)^3 & \epsilon \leq 1.2511 \\ -3.437 \exp(-\epsilon/0.75) & \epsilon \geq 1.2511 \end{cases}, \quad (5)$$

where  $\bar{R}$  is called the mean curvature radius, and it is dependent on the form of both nuclei. It can be expressed as:

$$\bar{R} = \frac{C_1 C_2}{C_1 + C_2}, \quad (6)$$

$C_1$  and  $C_2$ , known as the Süssmann central radii, are calculated using

$$C_i = R_i - \left( \frac{b^2}{R_i} \right), \quad (7)$$

where  $R_i$  can be obtained with the aid of a semi-empirical formula in terms of mass number  $A_i$  [49]:

$$R_i = 1.28A_i^{1/3} - 0.76 + 0.8A_i^{-1/3}. \quad (8)$$

The penetration probability of the  $\alpha$  particle through the potential barrier can be determined with the aid of the WKB approximation [34, 51]:

$$P = \exp \left[ -\frac{2}{\hbar} \int_{R_i}^{R_o} \sqrt{2\mu[V(r) - Q]} dr \right], \quad (9)$$

where  $\mu = A_1 A_2 / A$  is the reduced mass,  $A_1$  and  $A_2$  are the mass numbers of emitted  $\alpha$  particle and daughter nucleus, respectively,  $A$  is the mass number of the parent nucleus,  $R_i$  and  $R_o$  are known as the classic turning points, obtained via:

$$V(R_i) = V(R_o) = Q. \quad (10)$$

The  $\alpha$ -decay half-life can finally be calculated via:

$$T_{1/2} = \frac{\ln 2}{\lambda}, \quad (11)$$

where  $\lambda = \nu P$ , and  $\nu = 10^{20} s^{-1}$  is known as the assault frequency.

## 2.2. Temperature dependent Coulomb and proximity potential model (CPPMT)

The temperature dependent proximity potentials can be written as:

$$V_P(r, T) = 4\pi\gamma(T)b(T)\bar{R}(T)\phi(\xi). \quad (12)$$

Here  $\phi(\xi)$  is still the universal function, the temperature dependent forms of the other parameters in equation (12) are given by [34, 52–54]:

$$\gamma(T) = \gamma(0) \left(1 - \frac{T - T_b}{T_b}\right)^{3/2}, \quad (13)$$

$$b(T) = b(0)(1 + 0.009T^2), \quad (14)$$

$$R(T) = R(0)(1 + 0.0005T^2). \quad (15)$$

Here  $T_b$  is the temperature that is associated with near Coulomb barrier energies. A different version of the temperature dependent surface energy coefficient given by  $\gamma(T) = \gamma(0)(1 - 0.07T)^2$  [34] has been used in this work. The temperature  $T$  (MeV) can be derived from: [55, 56]

$$E^* = E_{kin} + Q_{in} = \frac{1}{9}AT^2 - T, \quad (16)$$

where  $E^*$  denotes the parent nucleus excitation energy, and  $A$  is its mass number.  $Q_{in}$  represents the entrance channel Q-value of the system.  $E_{kin}$  is the kinetic energy of the  $\alpha$  particle emitted and can be obtained using [34]:

$$E_{kin} = (A_2/A)Q. \quad (17)$$

### 2.3. Royer empirical formula

In the year 2000, Royer [19] proposed an analytical formula for the calculation of the  $\alpha$ -decay half-lives of nuclei, by applying a fitting procedure to some  $\alpha$  emitters. The proposed formula did not contain dependence on the angular momentum carried by the  $\alpha$  particle. In the year 2010, Royer proposed an improved formula for calculating the  $\alpha$ -decay half-lives, which is explicitly dependent on the angular momentum ( $\ell$ ) carried by the  $\alpha$  particle. The angular momentum for even-even nuclei was taken to be zero. It was observed that the agreement with experimental data was better than what was earlier recorded. The proposed formula is given for even-even, even-odd, odd-even, and odd-odd nuclei as [20]:

$$\log_{10}[T] = -25.752 - 1.15055A^{\frac{1}{6}}\sqrt{Z} + \frac{1.5913Z}{\sqrt{Q}}, \quad (18)$$

$$\begin{aligned} \log_{10}[T] = & -27.750 - 1.1138A^{\frac{1}{6}}\sqrt{Z} + \frac{1.6378Z}{\sqrt{Q}} \\ & + \frac{1.7383 \times 10^{-6} ANZ[\ell(\ell+1)]^{\frac{1}{4}}}{Q} + 0.002457A[1 - (-1)^\ell], \end{aligned} \quad (19)$$

$$\log_{10}[T] = -27.915 - 1.1292A^{\frac{1}{6}}\sqrt{Z} + \frac{1.6531Z}{\sqrt{Q}} \quad (20)$$

$$+ \frac{8.9785 \times 10^{-7} ANZ[\ell(\ell+1)]^{\frac{1}{4}}}{Q} + 0.002513A[1 - (-1)^\ell],$$

$$\log_{10}[T] = -26.448 - 1.1023A^{\frac{1}{6}}\sqrt{Z} + \frac{1.5967Z}{\sqrt{Q}} \quad (21)$$

$$+ \frac{1.6961 \times 10^{-6} ANZ[\ell(\ell+1)]^{\frac{1}{4}}}{Q} + 0.00101A[1 - (-1)^\ell],$$

respectively. The short form of equations (18) – (21) can be written as:

$$\log_{10}[T] = a + bA^{\frac{1}{6}}\sqrt{Z} + \frac{cZ}{\sqrt{Q}} + \frac{d \times 10^{-6} ANZ[\ell(\ell+1)]^{\frac{1}{4}}}{Q} + eA[1 - (-1)^\ell], \quad (22)$$

where  $a, b, c, d, e$  are the coefficients given in equations (18) – (21) for even-even, even-odd, odd-even, and odd-odd nuclei, respectively. For even-even nuclei,  $d = e = 0$ .

#### 2.4. New Ren B (NRB) formula

In 2018, Akrawy et al. [25] studied the influence of nuclear isospin and angular momentum on  $\alpha$ -decay half-lives. The existing Ren B formula by [57], were improved by including asymmetry and angular momentum terms. With the aid of least square fit and experimental values of 365 nuclei, the authors obtained new coefficients for the Ren B formula. The New Ren B formula yielded better results in the calculation of  $\alpha$ -decay half-lives than the existing Ren B formula, when compared with the experimental data [25]. The New Ren B formula is given as:

$$\log_{10} T_{1/2}^{NRB} = a\sqrt{\mu}Z_1Z_2Q^{-1/2} + b\sqrt{\mu Z_1Z_2} + c + dI + eI^2 + f[\ell(\ell+1)], \quad (23)$$

where  $\mu$  is the reduced mass and the nuclear isospin asymmetry  $I = \frac{N-Z}{A}$ . The two  $\alpha$ -decay empirical formulas used in this work are the Royer formula and the New Ren B formula.

#### 2.5. Artificial Neural Network (ANN)

ANN is a multilayer neural network made up of an input layer, hidden layers, and an output layer. We label the structure of our ANN network as  $[M_1, M_2, \dots, M_n]$ , where  $M_i$  is the number of neurons in the  $i$ th layer.

$i = 1$  denotes the input layer while  $i = n$  denotes the output layer. The outputs from the  $i$ th hidden layer are calculated using the formula:

$$h(\theta_i, X) = \text{ReLU}(0.01w^{(i)}h(\theta_{i-1}, X) + 0.01b^{(i)}), \quad (24)$$

where  $h(\theta_{i-1}, X)$  denotes the outputs from the previous layers,  $w^{(i)}$  and  $b^{(i)}$  represent the parameters of the network, and ReLU is the activation function used in the hidden layers. The ReLU is a non-linear function that helps improve the performance of the model. It has been chosen as the activation function for the hidden layers in this work, because of its ability to solve the problem of vanishing gradient. The outputs  $h(\theta_1, X)$  of the input layer are basically the input data  $X$ . For a regression problem like in our case, activation functions are not required in the output layer, therefore the output of the ANN network can be expressed as:

$$y = g(\theta, X) = w^{(n)}h(\theta_{n-1}, X) + b^{(n)}, \quad (25)$$

where  $\theta = \{w^{(1)}, b^{(1)}, \dots, w^{(n)}, b^{(n)}\}$  represent the network parameters,  $h(\theta_{n-1}, x)$  represent the outputs of the hidden layers, and  $X$  denote the inputs. In this work, ANN models have been trained to predict both half-life and  $Q_\alpha$  values for some neutron-deficient nuclei. For the ANN model trained to predict the half-lives,  $M_1 = 4$  (consisting the mass number, charge number, orbital angular momentum, and  $Q_\alpha$  values) and  $M_n = 1$ , and for the ANN model trained to predict  $Q_\alpha$  values,  $M_1 = 2$  (consisting the mass number and charge number of the nuclei) and  $M_n = 1$ . The output layer  $M_n = 1$  because we are dealing with a regression problem.

It is important to observe how well the ANN model performs during the training phase, a cost function is used to achieve this. The cost function evaluates the performance of the model by observing the difference between the predicted and actual values. Learning takes place by reducing the cost function to the barest minimum, this is achieved with the aid of an optimizing algorithm. Adam is one of the most widely used optimization algorithms. It has been employed in this work to derive the best values for the parameters in the ANN network, by modifying the parameters  $w^{(i)}$  and  $b^{(i)}$  for  $i = 1, \dots, n$  in the network until an acceptable value between the predicted and actual output is achieved. The root mean square error has been used as the cost function in this study. It can be expressed as:

$$\text{RMSE}(\theta) = \sqrt{\frac{1}{N} \sum_{i=1}^N \left[ Y_i^{\text{expt}} - g(\theta, X_i) \right]^2}, \quad (26)$$



where  $Y_i^{\text{expt}}$  denote the experimental values,  $g(\theta, X_i)$  are the predicted output values, and  $N$  is the size of the training data set.

In training the ANN model to predict the half-lives, a total number ( $N$ ) of 549 nuclei in the NUBASE2020 database have been used. As a result, a network structure of [4,50,100,50,1] has been chosen. During the training phase, the dataset was split into 80% train set and 20 % test set. The test set has been used to validate the performance of the trained model. The performance of the model can be improved, if necessary, by tweaking the parameters of the model before using it for predictions.

To predict the half-lives for unmeasured neutron-deficient nuclei, the  $Q_\alpha$  values are required as part of the input data. These unmeasured neutron-deficient nuclei have no experimental  $Q_\alpha$  values. The aid of machine learning is therefore sought to predict the  $Q_\alpha$  values, which can subsequently be used to calculate the half-lives of the unmeasured neutron-deficient nuclei. In order to achieve this, an ANN model is trained using about 1021  $Q_\alpha$  values of measured nuclei in the NUBASE2020 database. The dataset is also split into 80 % train set and 20 % test set. As a result of the number of instances of the data, a network structure of [2,120,120,120,1] has been chosen, and the performance accuracy is also determined using root mean square error.

### 3. Results and Discussion

The results of the calculations of the  $\alpha$ -decay half-lives of some neutron-deficient nuclei are presented and discussed here. The calculations have been carried out using Coulomb and proximity potential model (CPPM), temperature dependent Coulomb and proximity potential model (CPPMT), Royer empirical formula (Royer), new Ren B empirical formula (NRB), and trained artificial neural network (ANN).

The coefficients given in Ref. [20] for the Royer formula and Ref. [25] for the new Ren B formula were obtained with the aid of a fitting procedure applied to the  $\alpha$ -decay half-lives in previous NUBASE databases. In this study, new coefficients have been obtained for the two formulas by applying the least square fit scheme and using 549  $\alpha$  emitters in the NUBASE2020 database, containing 189 even-even, 150 even-odd, 117 odd-even and 93 odd-odd nuclei. The new coefficients obtained are given in Table 1 for Royer formula and Table 2 for new Ren B (NRB) formula. The root mean square error (RMSE) values obtained are 0.5411 for Royer formula, and 0.5538 for NRB formula.

Table 1: New coefficients for the Royer formula.

Nuclei	$a$	$b$	$c$	$d$	$e$
even-even	-25.5993	-1.1362	1.5771	$0.0000 \times 10^0$	$0.0000 \times 10^0$
even-odd	-25.0031	-1.1327	1.5622	$6.9116 \times 10^{-7}$	$1.7000 \times 10^{-3}$
odd-even	-24.3063	-1.1861	1.5787	$9.7862 \times 10^{-7}$	$6.3120 \times 10^{-5}$
odd-odd	-25.9529	-1.1088	1.5848	$9.7423 \times 10^{-7}$	$-9.6530 \times 10^{-5}$

Table 2: New coefficients for the new Ren B formula.

Nuclei	$a$	$b$	$c$	$d$	$e$	$f$
even-even	0.4095	-1.4111	-15.2260	8.6687	-49.5989	0.0000
even-odd	0.4095	-1.3815	-14.8570	-9.5116	27.5012	0.0323
odd-even	0.4203	-1.4093	-15.3943	-7.2587	07.1358	0.0298
odd-odd	0.4135	-1.4380	-14.5336	1.7049	01.2728	0.0086

To calculate the  $\alpha$ -decay half-lives for some neutron-deficient nuclei using ANN, the algorithm is trained using the data of 549  $\alpha$  emitters. The train set contains 439 nuclei while the test set contains 110 nuclei. After training and optimizations, the values of the root mean square errors obtained for the train and test sets are shown in Table 3.

Table 3: The root mean square errors ( $\sigma$ ) obtained for the training set and test set after training ANN to predict the half-lives.

Artificial Neural Network (ANN)	$\sigma$
Train	0.3876
Test	0.5719

Having successfully trained the ANN model to predict  $\alpha$ -decay half-lives, the trained ANN model, CPPM, CPPMT, Royer, and NRB are now used to calculate the  $\alpha$ -decay half-lives of some neutron-deficient nuclei. Table 4 presents the results of the calculations. It can be observed that the values obtained from the five models are in good agreements with the experimental values.

Table 4: The Experimental and predicted  $\log[T_{1/2}(s)]$  values for 69 neutron-deficient nuclei within the range of  $80 \leq Z \leq 118$ .

A	Z	$Q_\alpha$	$\ell$	$\log[T_{1/2}(s)]$					
				Expt	CPPM	CPPMT	Royer	NRB	ANN
171	80	7.6677	2	-4.1549	-3.8676	-3.6663	-3.5599	-3.6724	-3.9863
172	80	7.5238	0	-3.6364	-3.7166	-3.5231	-3.5659	-3.6714	-3.2377
173	80	7.3780	0	-3.0969	-3.2855	-3.0928	-2.9044	-3.0393	-2.8762
174	80	7.2333	0	-2.6990	-2.8430	-2.6511	-2.6975	-2.7415	-2.4969
177	81	7.0670	0	-1.6081	-1.9244	-1.7315	-1.4987	-1.5908	-1.5784
178	81	7.0200	2	-0.3859	-1.5200	-1.3210	-0.8672	-1.3056	-0.5979
179	81	6.7091	0	-0.1377	-0.6898	-0.4987	-0.2800	-0.3497	-0.3485
178	82	7.7895	0	-3.6021	-3.8289	-3.6332	-3.6638	-3.7310	-3.3282
179	82	7.5961	2	-2.5686	-3.0065	-2.8046	-2.6684	-2.8173	-2.6574
180	82	7.4187	0	-2.3872	-2.7246	-2.5304	-2.5653	-2.5799	-2.3492
187	83	7.7791	5	-1.4318	-2.3051	-2.0748	-2.6682	-2.4127	-2.5861
186	84	8.5012	0	-4.4685	-5.2045	-5.0084	-5.0413	-5.0398	-4.5078
188	84	8.0823	0	-3.5686	-4.0855	-3.8900	-3.9232	-3.8862	-3.5392
189	84	7.6943	2	-2.4559	-2.6921	-2.4901	-2.3272	-2.4853	-2.4598
191	85	7.8223	5	-2.6778	-1.7272	-1.4932	-2.0419	-1.7761	-1.9592
193	86	8.0400	2	-2.9393	-3.0276	-2.8220	-2.6313	-2.7971	-2.8824
194	86	7.8624	0	-3.1079	-2.7551	-2.5566	-2.5785	-2.5265	-2.1815
196	86	7.6167	0	-2.3279	-2.0125	-1.8148	-1.8480	-1.7757	-1.6018
197	87	7.8964	3	-2.6383	-2.0219	-1.8081	-1.6564	-1.8255	-2.5173
199	87	7.8168	0	-2.1805	-2.3000	-2.1008	-1.9129	-1.9754	-1.8068
201	88	8.0015	0	-1.6990	-2.5137	-2.3127	-2.1173	-2.1914	-1.9148
202	88	7.8803	0	-2.3872	-2.1527	-1.9520	-1.9762	-1.9010	-1.6470
203	88	7.7363	0	-1.4437	-1.7082	-1.5077	-1.3335	-1.3730	-1.3051
204	88	7.6366	0	-1.2218	-1.3973	-1.1971	-1.2360	-1.1520	-1.0045
205	89	8.0932	0	-1.0969	-2.4696	-2.2674	-2.0889	-2.1312	-1.8515
206	89	7.9583	0	-1.6021	-2.0673	-1.8653	-1.3750	-1.3382	-1.5490
207	89	7.8449	0	-1.5086	-1.7224	-1.5206	-1.3574	-1.3750	-1.2760
208	89	7.7286	0	-1.0132	-1.3595	-1.1579	-0.6785	-0.5748	-0.9364
208	90	8.2020	0	-2.6198	-2.4620	-2.2584	-2.2735	-2.1985	-1.8051
210	90	8.0690	0	-1.7959	-2.0839	-1.8806	-1.9085	-1.8301	-1.5345
211	90	7.9375	0	-1.3188	-1.6844	-1.4812	-1.3145	-1.2960	-1.2046
212	91	8.4108	0	-2.2366	-2.7663	-2.5615	-2.0529	-2.0004	-2.0309
213	91	8.3844	0	-2.1308	-2.7031	-2.4985	-2.3432	-2.3619	-1.9940
215	91	8.2361	0	-1.8539	-2.2864	-2.0819	-1.9417	-1.9427	-1.6860
216	91	8.0993	2	-0.9788	-1.6378	-1.4265	-0.7237	-0.9561	-0.9593
216	92	8.5306	0	-2.1612	-2.8024	-2.5962	-2.6148	-2.5441	-2.0390

Contd

Table 4 – *Contd*

A	Z	$Q_\alpha$	$\ell$	$\log[T_{1/2}(s)]$					
				Expt	CPPM	CPPMT	Royer	NRB	ANN
218	92	8.7748	0	-3.4510	-3.5262	-3.3208	-3.3519	-3.2938	-2.6983
219	93	9.2075	0	-3.2441	-4.3515	-4.1450	-4.0041	-4.0452	-3.4962
223	93	9.6504	0	-5.6021	-5.5184	-5.3139	-5.2123	-5.2794	-5.3452
225	93	8.8182	0	-2.1871	-3.3793	-3.1725	-3.0745	-3.0632	-2.6083
228	94	7.9402	0	0.3222	-0.3549	-0.1446	-0.2144	-0.1754	0.2239
229	94	7.5980	2	2.2601	1.0589	1.2762	1.5247	1.5507	1.1252
230	94	7.1785	0	2.0212	2.3818	2.5922	2.4671	2.5020	2.3075
231	94	6.8386	0	3.5987	3.7556	3.9658	3.9517	4.2917	3.6338
234	96	7.3653	0	2.2846	2.4459	2.6601	2.5551	2.6082	2.4021
236	96	7.0670	0	3.3554	3.6116	3.8260	3.6812	3.7185	3.5425
237	98	8.2200	2	0.0580	0.3857	0.6102	0.9290	0.9302	0.8602
240	98	7.7110	0	1.6119	1.8946	2.1129	2.0218	2.0646	1.9214
242	99	8.1601	2	1.4945	0.9121	1.1390	2.0714	1.8378	1.4903
243	100	8.6892	1	-0.5954	-0.5957	-0.3724	0.8667	0.0249	-0.0970
247	101	8.7644	1	0.0755	-0.5084	-0.2831	0.2091	0.0054	0.0711
251	102	8.7517	0	-0.0160	-0.2224	0.0029	0.1319	0.4853	-0.0580
254	103	8.8218	3	1.2237	0.3384	0.5804	1.4500	1.1793	0.9884
255	104	9.0555	1	0.4896	-0.4050	-0.1740	1.1434	0.3150	0.6843
256	104	8.9257	0	0.3282	-0.0911	0.1380	0.1053	0.1402	0.1547
256	105	9.3361	2	0.3854	-0.7522	-0.5153	0.5411	0.2246	0.4760
259	106	9.7651	2	-0.3958	-1.6609	-1.4233	-0.9860	-0.9367	-0.4093
260	106	9.9006	0	-1.7678	-2.2570	-2.0268	-2.0209	-1.9894	-1.9146
261	106	9.7137	2	-0.7292	-1.5412	-1.3030	-0.8716	-0.7890	-0.2402
261	107	10.5002	3	-1.8928	-3.0653	-2.8213	-2.4141	-2.5845	-1.7629
265	108	10.4703	0	-2.7077	-3.1370	-2.9048	-2.6917	-2.3532	-2.5175
266	108	10.3457	0	-2.4037	-2.8320	-2.5991	-2.5868	-2.5642	-2.3619
267	110	11.7768	0	-5.0000	-5.5563	-5.3268	-5.0711	-4.8241	-4.7157
270	110	11.1170	0	-3.6882	-4.1269	-3.8935	-3.8621	-3.8351	-3.3006
286	114	10.3551	0	-0.6569	-1.1086	-0.8609	-0.8646	-0.8471	-0.9908
288	114	10.0765	0	-0.1851	-0.3534	-0.1036	-0.1337	-0.1342	0.0531
290	116	10.9968	0	-2.0458	-2.1865	-1.9378	-1.9130	-1.8826	-1.9792
292	116	10.7912	0	-1.7959	-1.6805	-1.4300	-1.4259	-1.4144	-1.5953
294	118	11.8673	0	-3.1549	-3.6977	-3.4498	-3.4021	-3.3665	-3.0170

Figure (1) shows the plots of the  $\log[T_{1/2}(s)]$  values for the 69 neutron-deficient nuclei obtained from using the various models. The experimental data are included for comparison. It is observed from the plot that the predicted values agree with the values obtained from experiment.

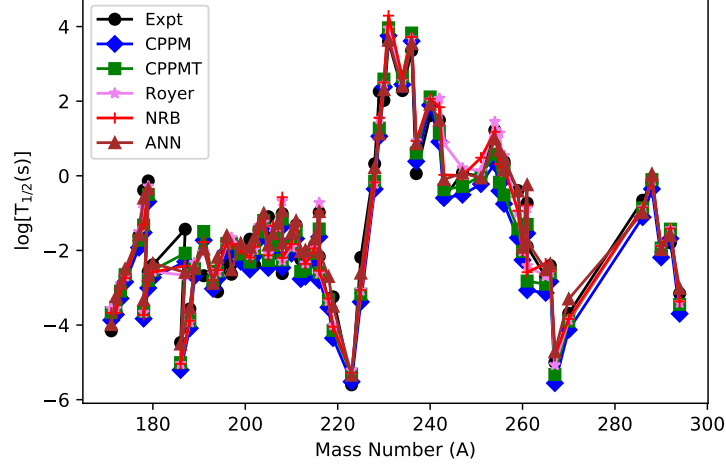


Fig. 1: Plots of the experimental and theoretically calculated  $\alpha$ -decay half-lives for some neutron-deficient nuclei using CPPM, CPPMT, Royer, NRB, and ANN models.

In order to quantitatively evaluate the performance of the models, the root mean square error (RMSE) is calculated. The experimental  $\alpha$ -decay half-lives are retrieved from Refs. [44, 45]. Table 5 presents the computed root mean square error for all the models. It can be observed that the ANN model gives the lowest RMSE, with a value of 0.3843. The CPPMT (RMSE = 0.4963) is found to give lower RMS error compared to the CPPM (RMSE = 0.5946), indicating the importance of the use of temperature dependent potential. The NRB formula is also found to give lower RMSE value than the Royer formula. The calculated temperature values (in MeV) for the neutron-deficient nuclei in the CPPMT model are plotted with respect to the mass number (A) of these nuclei in Figure (2).

Table 5: The calculated RMSE values obtained for the neutron-deficient nuclei using CPPM, CPPMT, Royer, NRB, and ANN.

Models (Formulas)	$\sigma$
CPPM	0.5946
CPPMT	0.4963
Royer	0.4608
NRB	0.4413
ANN	0.3843

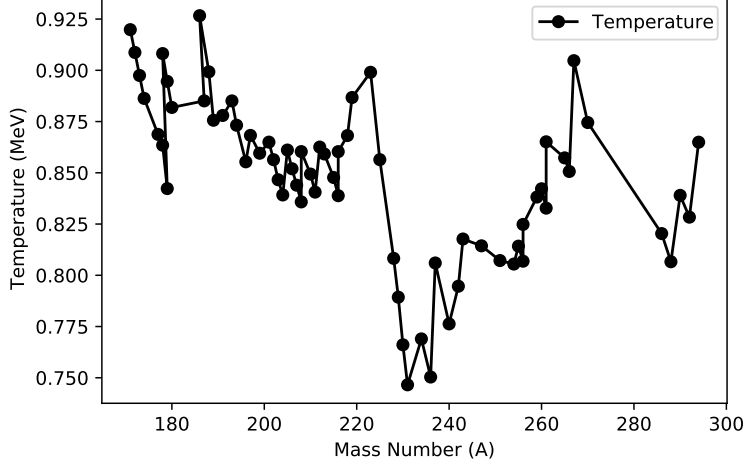


Fig. 2: Plot of the calculated temperature (MeV) values in the CPPMT for 69 neutron-deficient nuclei with respect to their mass number (A).

The energy released ( $Q_\alpha$ ) during an  $\alpha$ -decay process is one of the important input parameters required to calculate  $\alpha$ -decay half-lives. To predict the half-lives of  $\alpha$ -decay from unmeasured neutron-deficient nuclei, the  $Q_\alpha$  values are required. Previously the Weizsäcker-Skyrme-4 (WS4) and Weizsäcker-Skyrme-4+RBF (WS4+RBF) [46] formulas were used to predict the  $Q_\alpha$  values of unmeasured neutron-deficient nuclei [29]. However in this work, we are motivated to use ANN to predict the  $Q_\alpha$  values, following its success in predicting the  $\alpha$ -decay half-lives. To achieve this, an artificial neural network (ANN) is trained using 1021  $Q_\alpha$  values of measured nuclei in the NUBASE2020 database. The  $Q_\alpha$  values are again split into train (80 % of data) and test (20 % of data) sets. Procedure similar to that followed in the training of the half-lives is followed. After training and optimizations, the root mean square errors obtained on the train and test sets are given in Table 6.

Table 6: The  $\sigma$  values between the experimental and predicted  $Q_\alpha$  values for the training and test set.

Artificial Neural Network (ANN)	$\sigma$
Train	0.1684
Test	0.1802

In order to compare the performance of the ANN predictions of  $Q_\alpha$  values with existing theories, we have used the ANN model to predict  $Q_\alpha$  values for 69 neutron-deficient nuclei. The outputs are compared with the predictions of WS4 and WS4+RBF models. Table 7 presents the root mean square error values obtained when the predictions of ANN, WS4, and WS4+RBF are compared with experimental values. With a standard deviation value of 0.1475, the ANN model is found to give a slightly lower RMSE value than WS4+RBF theoretical model. The WS4+RBF, as expected, performs better than the WS4 formula. Figure (3) shows the plots of the  $Q_\alpha$  values predicted by WS4, WS4+RBF, and ANN models for the neutron-deficient nuclei.

Table 7: The computed root mean square errors ( $\sigma$ ) obtained using WS4, WS4+RBF, and ANN models.

Models	$\sigma$
WS4	0.2038
WS4+RBF	0.1565
ANN	0.1475

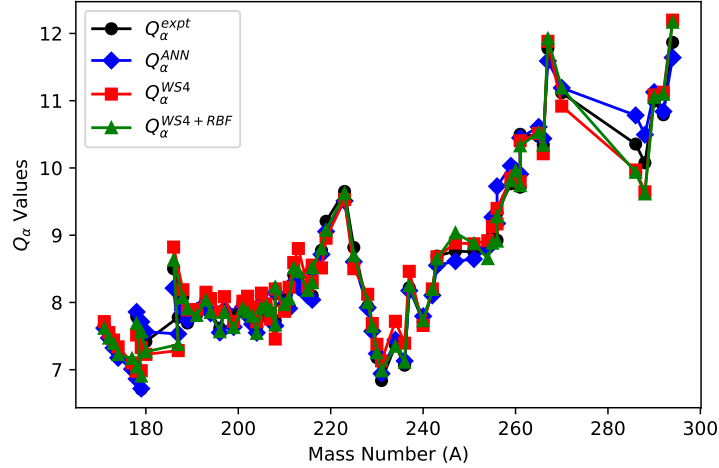


Fig. 3: Plots of the experimental and predicted  $Q_\alpha$  values for 69 neutron-deficient nuclei using WS4, WS4+RBF, and ANN models.

Since the trained ANN model performed very well in predicting the  $Q_\alpha$

values, we are now on track to predict the  $\alpha$ -decay half-lives of unmeasured neutron-deficient nuclei. The  $Q_\alpha$  values predicted by the ANN model (denoted as  $Q_\alpha^{ANN}$ ) will be used as part of the input values. The  $\alpha$ -decay half-lives of the neutron-deficient nuclei within the range of  $80 \leq Z \leq 120$  and  $169 \leq A \leq 296$  will then be predicted using CPPM, CPPMT, Royer, NRB, and the trained artificial neural network (denoted as  $T^{ANN}$ ) models. The angular momentum  $\ell$  carried by the emitted  $\alpha$  particle has been taken to be zero for all nuclei. Table 8 presents the predicted half-lives for  $\alpha$ -decay of the 126 unmeasured neutron-deficient nuclei using the various theoretical models and  $T^{ANN}$ . The third to fifth columns of the Table show the  $Q_\alpha$  values predicted by the WS4 ( $Q_\alpha^{WS4}$ ), WS4+RBF ( $Q_\alpha^{WS4+RBF}$ ), and ANN ( $Q_\alpha^{ANN}$ ) models. The sixth to tenth columns show the predictions using CPPM, CPPMT, Royer, NRB, and  $T^{ANN}$ . The last column is the previous theoretical calculations of Cui et al. [29] using generalized liquid drop model (GLDM). A careful observation of the values indicate that the results are close to that predicted earlier by Cui et al. [29]. Figure (4) shows the plots of the predicted  $\log[T_{1/2}(s)]$  values using the various models.

Table 8: The predicted  $\log[T_{1/2}(s)]$  values for 126 unmeasured neutron-deficient nuclei within the range of  $80 \leq Z \leq 120$  using  $Q_\alpha$  values predicted by ANN ( $Q_\alpha^{ANN}$ ). Previous theoretical predictions by Cui et al. [29] using GLDM are included for comparison. The  $Q_\alpha^{WS4+RBF}$  values have been taken from [46]

A	Z	$Q_\alpha^{WS4}$	$Q_\alpha^{WS4+RBF}$	$Q_\alpha^{ANN}$	$\log[T_{1/2}(s)]$					
					CPPM	CPPMT	Royer	NRB	$T^{ANN}$	GLDM
169	80	7.8870	7.7235	7.9151	-4.7990	-4.6030	-4.3998	-4.5162	-4.1667	-4.2020
170	80	7.8490	7.7214	7.7667	-4.3969	-4.2017	-4.2443	-4.4235	-3.8227	-4.4034
174	81	7.5690	7.6406	7.4513	-3.1224	-2.9271	-2.5043	-2.8317	-2.8110	-2.9245
175	81	7.4680	7.5169	7.3018	-2.6660	-2.4715	-2.2307	-2.3293	-2.3871	-2.7747
176	82	7.8730	8.1468	8.1580	-4.8419	-4.6449	-4.6765	-4.8072	-4.2548	-3.6289
177	82	7.6880	7.8397	8.0084	-4.4440	-4.2477	-4.0379	-4.1846	-3.9177	-2.2000
182	83	8.3450	8.4631	8.2967	-4.9568	-4.7610	-4.3330	-4.5801	-4.4132	-3.1180
183	83	8.0580	8.2330	8.1659	-4.6157	-4.4205	-4.2003	-4.3560	-4.1222	-3.3507
184	84	9.1510	9.2195	8.5091	-5.1886	-4.9912	-5.0178	-5.0579	-4.6249	-6.6498
185	84	8.9660	8.8820	8.3642	-4.8188	-4.6219	-4.4072	-4.5643	-4.2987	-5.5258
189	85	8.4560	8.0567	8.2046	-4.0686	-3.8707	-3.6550	-3.7821	-3.6884	-4.1035
190	85	8.1530	7.9320	8.0399	-3.6110	-3.4135	-2.9546	-3.1026	-3.2766	-2.9747
191	86	8.4930	8.3920	8.3470	-4.1255	-3.9259	-3.7059	-3.8478	-3.7540	-3.9626
192	86	8.2250	8.1818	8.1697	-3.6383	-3.4390	-3.4530	-3.4299	-3.2933	-3.7959
195	87	8.3190	8.1319	8.1451	-3.2338	-3.0331	-2.8230	-2.9083	-2.8545	-3.2933
196	87	8.2120	7.8721	8.0140	-2.8593	-2.6590	-2.1740	-2.2908	-2.4014	-3.0205
199	88	8.1950	8.1145	8.1821	-3.0260	-2.8243	-2.6138	-2.7142	-2.5563	-2.7144

*Contd*



Table 8 – *Contd*

A	Z	$Q_{\alpha}^{WS4}$	$Q_{\alpha}^{WS4+RBF}$	$Q_{\alpha}^{ANN}$	$\log[T_{1/2}(s)]$					
					CPPM	CPPMT	Royer	NRB	ANN	GLDM
200	88	8.0320	8.0609	8.0561	-2.6643	-2.4629	-2.4759	-2.4154	-2.1597	-2.6271
203	89	8.5130	8.3122	8.2246	-2.8343	-2.6316	-2.4408	-2.4945	-2.3111	-3.4123
204	89	8.3610	8.0277	8.0985	-2.4701	-2.2676	-1.7684	-1.7958	-1.9773	-3.1361
206	90	8.5770	8.4303	8.3932	-2.9993	-2.7951	-2.7990	-2.7347	-2.4549	2.3655
207	90	8.3660	8.2410	8.2671	-2.6424	-2.4384	-2.2359	-2.2877	-2.1209	-2.6925
209	91	8.5970	8.7452	8.5621	-3.1601	-2.9546	-2.7734	-2.8115	-2.5994	-3.1007
210	91	8.3590	8.5251	8.4361	-2.8108	-2.6054	-2.0869	-2.0940	-2.2659	-2.5498
213	92	8.8220	8.7026	8.6599	-3.1307	-2.9241	-2.7112	-2.7436	-2.5706	-3.4214
214	92	9.1570	8.6648	8.5962	-2.9633	-2.7568	-2.7634	-2.6916	-2.4186	-4.5214
221	93	10.5510	10.5627	10.2851	-6.9486	-6.7464	-6.6515	-6.7726	-6.9742	-6.7122
222	93	10.0770	9.9496	9.9162	-6.1337	-5.9301	-5.4600	-5.3107	-6.1410	-5.7932
226	94	8.7920	8.9110	8.6969	-2.6852	-2.4761	-2.5152	-2.4735	-2.2448	-2.8894
227	94	8.5180	8.5648	8.2903	-1.4747	-1.2649	-1.1222	-0.9567	-1.0712	-2.0070
228	95	8.7070	8.6537	8.3877	-1.4136	-1.2020	-0.6793	-0.4516	-0.9432	-2.3605
229	95	8.3210	8.1832	8.0231	-0.2536	-0.0417	0.0468	0.1892	0.1426	-1.1561
231	96	8.1600	7.9503	7.9165	0.4742	0.6881	0.8114	1.0090	0.8291	-0.3556
232	96	7.9950	7.7965	7.7383	1.0864	1.3004	1.2336	1.2970	1.3111	0.0607
232	97	8.6200	8.3928	8.2418	-0.2396	-0.0240	0.5248	0.7347	0.1942	-1.7167
233	97	8.4670	8.2118	8.1018	0.2113	0.4270	0.5153	0.7029	0.5818	-1.0482
235	98	8.8030	8.5756	8.4027	-0.4168	-0.1994	-0.0400	0.1426	-0.0364	-1.8182
236	98	8.6370	8.4122	8.2898	-0.0640	0.1535	0.1218	0.1889	0.2640	-1.3645
238	99	8.8710	8.8323	8.5907	-0.6741	-0.4551	0.1134	0.3412	-0.3543	-1.9830
239	99	8.6660	8.6226	8.4779	-0.3299	-0.1107	-0.0288	0.1800	-0.0539	-1.0434
239	100	9.3180	9.2752	9.0044	-1.5734	-1.3532	-1.1562	-0.9931	-1.1934	-2.6904
240	100	9.1130	9.0738	8.8916	-1.2518	-1.0313	-1.0318	-0.9633	-0.9505	-2.0964
243	101	9.1940	9.2682	9.0886	-1.5116	-1.2896	-1.1940	-0.9960	-1.2614	-1.8962
244	101	9.2850	9.3598	8.9778	-1.1967	-0.9744	-0.3868	-0.1428	-1.0136	-2.3125
246	102	10.0020	10.0677	9.2872	-1.7673	-1.5438	-1.5352	-1.4744	-1.5546	-3.9101
247	102	9.8410	9.9120	9.1764	-1.4601	-1.2362	-1.0525	-0.8081	-1.3344	-3.1068
249	103	9.8930	9.9942	9.4866	-2.0175	-1.7924	-1.7061	-1.4856	-1.8338	-2.8153
250	103	9.5980	9.6889	9.3756	-1.7168	-1.4914	-0.8859	-0.6261	-1.5944	-1.9626
251	104	9.8240	9.8773	9.7971	-2.5478	-2.3217	-2.1050	-1.8805	-2.2510	-2.2034
252	104	9.5560	9.5519	9.6860	-2.2597	-2.0332	-2.0169	-1.9635	-2.0149	-1.9706
253	105	9.8040	9.7829	10.1091	-3.0566	-2.8296	-2.7369	-2.5234	-2.6619	-1.6840
254	105	9.5950	9.5263	9.9977	-2.7794	-2.5520	-1.9171	-1.7028	-2.4251	-0.9586
256	106	9.7470	9.6551	10.3055	-3.2651	-3.0368	-2.9989	-2.9419	-2.8264	-1.7190
257	106	9.7110	9.6039	10.1769	-2.9495	-2.7206	-2.4966	-2.2387	-2.5495	-0.5361
258	107	10.2050	10.1217	10.6190	-3.7425	-3.5134	-2.8536	-2.6830	-3.2131	-1.5421
259	107	10.2430	10.1697	10.5628	-3.6176	-3.3883	-3.3081	-3.0738	-3.1183	-1.4237
261	108	10.9560	10.8824	10.9797	-4.3210	-4.0915	-3.8401	-3.6084	-3.7525	-2.8386
262	108	11.0170	10.9343	10.9286	-4.2137	-3.9840	-3.9429	-3.8976	-3.6363	-3.8570
263	109	11.7210	11.5862	11.4034	-4.9987	-4.7693	-4.6934	-4.4802	-4.4301	-4.2336
264	109	11.6690	11.5516	11.3524	-4.8980	-4.6682	-4.0033	-3.8277	-4.3126	-5.0141

*Contd*

Table 8 – *Contd*

A	Z	$Q_{\alpha}^{WS4}$	$Q_{\alpha}^{WS4+RBF}$	$Q_{\alpha}^{ANN}$	$\log[T_{1/2}(s)]$					
					CPPM	CPPMT	Royer	NRB	ANN	GLDM
261	110	12.1470	12.0874	11.9956	-5.9378	-5.7091	-5.4160	-5.2881	-5.4567	-5.1707
262	110	12.2240	12.1576	11.9611	-5.8797	-5.6510	-5.5802	-5.5186	-5.3783	-5.5287
263	110	12.3370	12.2642	11.9268	-5.8216	-5.5928	-5.3114	-5.1460	-5.3003	-5.0391
264	110	12.3870	12.3230	11.8801	-5.7369	-5.5079	-5.4476	-5.3933	-5.1938	-5.9788
265	110	12.3340	12.2357	11.8285	-5.6413	-5.4121	-5.1430	-4.9368	-5.0755	-5.1630
266	110	12.1720	12.1327	11.7170	-5.4173	-5.1875	-5.1366	-5.0907	-4.8168	-5.6840
266	111	12.7280	12.6966	12.3057	-6.3402	-6.1116	-5.4305	-5.3582	-5.8294	-6.7167
267	111	12.5450	12.5439	12.1922	-6.1250	-5.8958	-5.8310	-5.6302	-5.5700	-5.2807
268	111	12.2400	12.3038	12.0656	-5.8794	-5.6495	-4.9710	-4.8395	-5.2807	-5.7645
269	111	11.9250	12.0929	11.9402	-5.6315	-5.4008	-5.3436	-5.1125	-4.9929	-4.1785
270	111	11.6370	11.8923	11.8203	-5.3906	-5.1592	-4.4851	-4.2940	-4.7148	-4.4802
271	111	11.3730	11.5357	11.6883	-5.1189	-4.8867	-4.8393	-4.5764	-4.4084	-3.1158
270	112	12.2850	12.4256	12.4175	-6.3279	-6.0980	-6.0412	-5.9927	-5.7475	-5.2774
271	112	12.0610	12.2550	12.2921	-6.0896	-5.8589	-5.5892	-5.3513	-5.4609	-4.1574
272	112	11.8620	12.0421	12.1730	-5.8598	-5.6283	-5.5780	-5.5372	-5.1887	-4.5171
273	112	11.6400	11.8677	12.0494	-5.6163	-5.3841	-5.1265	-4.8383	-4.9047	-3.4559
274	112	11.5480	11.5164	11.9118	-5.3387	-5.1055	-5.0631	-5.0325	-4.5852	-4.0048
275	112	11.7410	11.7436	11.7868	-5.0826	-4.8486	-4.6052	-4.2638	-4.2952	-3.7825
272	113	12.5120	12.7064	12.7716	-6.7611	-6.5313	-5.8437	-5.7540	-6.2190	-5.8827
273	113	12.3250	12.4612	12.6459	-6.5315	-6.3009	-6.2548	-6.0278	-5.9319	-4.4584
274	113	12.0840	12.1525	12.5365	-6.3296	-6.0983	-5.4128	-5.2648	-5.6819	-5.0794
275	113	11.9340	12.0250	12.4338	-6.1376	-5.9056	-5.8677	-5.6133	-5.4471	-3.7878
276	113	12.0640	12.0436	12.3179	-5.9161	-5.6834	-5.0025	-4.7967	-5.1825	-4.9914
277	113	12.2010	12.1090	12.1994	-5.6852	-5.4516	-5.4229	-5.1381	-4.9113	-4.4283
278	114	12.5190	12.5039	12.7329	-6.4816	-6.2495	-6.2041	-6.1706	-5.7936	-5.3497
279	114	12.4300	12.3872	12.5629	-6.1597	-5.9263	-5.6689	-5.3498	-5.4047	-4.5918
280	114	12.2260	12.1816	12.3383	-5.7192	-5.4842	-5.4419	-5.4159	-4.8911	-4.8729
281	114	11.8160	11.7729	12.0572	-5.1449	-4.9080	-4.6629	-4.2787	-4.2893	-3.4660
282	114	11.3780	11.3363	11.7095	-4.3998	-4.1606	-4.1222	-4.0993	-3.6364	-3.1518
283	114	10.8790	10.8393	11.3618	-3.6170	-3.3755	-3.1532	-2.6909	-3.0090	-1.4342
281	115	12.2030	12.1640	12.8276	-6.4237	-6.1899	-6.1691	-5.8820	-5.6719	-3.8633
282	115	11.7770	11.7367	12.6022	-5.9924	-5.7570	-5.0622	-4.8337	-5.1561	-3.9393
283	115	11.3240	11.2842	12.3640	-5.5215	-5.2844	-5.2660	-4.9299	-4.6075	-2.0953
284	115	10.9330	10.8941	12.0163	-4.8003	-4.5608	-3.8615	-3.5616	-3.9542	-1.9666
285	115	10.7300	10.6920	11.6687	-4.0433	-3.8014	-3.7881	-3.3798	-3.3014	-0.7282
286	115	10.5010	10.4646	11.3257	-3.2589	-3.0148	-2.3179	-1.9406	-2.7463	-0.7932
283	116	12.1070	12.0713	13.0928	-6.6803	-6.4461	-6.1769	-5.8667	-5.9399	-3.4248
284	116	11.8320	11.7950	12.8660	-6.2570	-6.0213	-5.9681	-5.9302	-5.4211	-3.4535
285	116	11.5490	11.5115	12.6434	-5.8290	-5.5916	-5.3313	-4.9603	-4.9118	-2.3188
286	116	11.3120	11.2755	12.3235	-5.1861	-4.9464	-4.8944	-4.8603	-4.2727	-2.3585
287	116	11.2840	11.2478	11.9755	-4.4526	-4.2105	-3.9658	-3.5206	-3.6192	-1.7959
288	116	11.2900	11.2551	11.6278	-3.6833	-3.4388	-3.3945	-3.3610	-3.0211	-2.4168
285	117	12.4450	12.4112	13.3513	-6.9169	-6.6824	-6.6684	-6.3692	-6.1928	-3.8153

*Contd*

Table 8 – *Contd*

A	Z	$Q_{\alpha}^{WS4}$	$Q_{\alpha}^{WS4+RBF}$	$Q_{\alpha}^{ANN}$	$\log[T_{1/2}(s)]$					
					CPPM	CPPMT	Royer	NRB	ANN	GLDM
286	117	12.2670	12.2324	13.1308	-6.5154	-6.2793	-5.5673	-5.3732	-5.6882	-4.5986
287	117	12.0520	12.0169	12.9076	-6.0969	-5.8591	-5.8452	-5.4999	-5.1777	-3.1215
288	117	11.9820	11.9472	12.6317	-5.5592	-5.3193	-4.6020	-4.3407	-4.5929	-3.9872
289	117	11.9870	11.9523	12.2830	-4.8475	-4.6051	-4.5925	-4.1833	-3.9383	-3.1079
290	117	11.8390	11.8056	11.9347	-4.1017	-3.8569	-3.1358	-2.7982	-3.3030	-3.6326
288	118	12.6160	12.5833	13.3997	-6.7737	-6.5373	-6.4756	-6.4262	-5.9648	-4.4597
289	118	12.5920	12.5590	13.1729	-6.3587	-6.1206	-5.8473	-5.4854	-5.4461	-3.9586
290	118	12.6010	12.5675	12.9401	-5.9191	-5.6792	-5.6172	-5.5723	-4.9134	-4.5258
291	118	12.4200	12.3873	12.5911	-5.2286	-4.9862	-4.7235	-4.2933	-4.2585	-3.7190
292	118	12.2400	12.2080	12.2574	-4.5377	-4.2928	-4.2324	-4.1871	-3.6322	-3.8794
293	118	12.2420	12.2100	11.9355	-3.8411	-3.5939	-3.3518	-2.8461	-3.1053	-3.4522
289	119	13.1750	13.1266	13.8570	-7.3501	-7.1149	-7.1084	-6.7948	-6.6725	-4.6655
290	119	13.0670	13.0351	13.6591	-7.0071	-6.7703	-6.0430	-5.8820	-6.2197	-5.7799
291	119	13.0480	13.0161	13.4411	-6.6179	-6.3795	-6.3717	-6.0151	-5.7210	-4.5376
292	119	12.9020	12.8696	13.2155	-6.2030	-5.9629	-5.2294	-5.0040	-5.2050	-5.4248
293	119	12.7150	12.6834	12.9101	-5.6173	-5.3748	-5.3666	-4.9556	-4.5994	-4.0057
294	119	12.7260	12.6947	12.5855	-4.9678	-4.7228	-3.9822	-3.6844	-3.9907	-5.0985
291	120	13.5090	13.4787	14.1035	-7.5470	-7.3114	-7.0234	-6.7247	-6.8978	-4.9872
292	120	13.4680	13.4370	13.9114	-7.2213	-6.9842	-6.9149	-6.8539	-6.4583	-5.4271
293	120	13.4000	13.3695	13.7083	-6.8678	-6.6291	-6.3453	-5.9911	-5.9938	-4.8996
294	120	13.2420	13.2109	13.4888	-6.4741	-6.2337	-6.1627	-6.1055	-5.4916	-5.1720
295	120	13.2720	13.2410	13.2420	-6.0166	-5.7743	-5.4978	-5.0826	-4.9614	-4.8297
296	120	13.3430	13.3124	12.9143	-5.3822	-5.1373	-5.0653	-5.0094	-4.3504	-5.4609

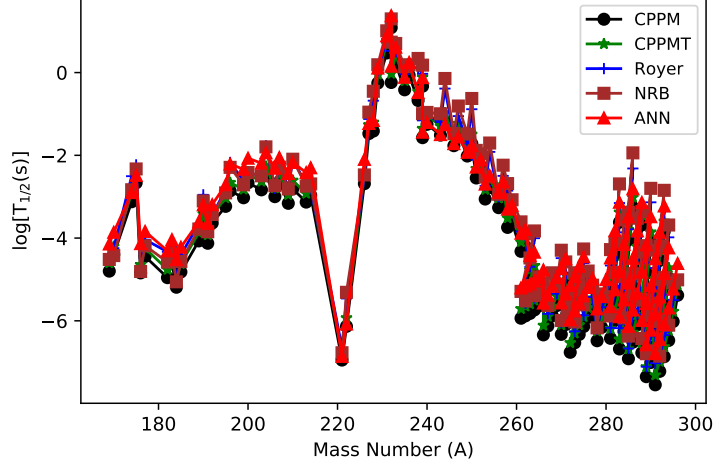


Fig. 4: Plots of the predicted  $\alpha$ -decay half-lives for the neutron-deficient nuclei using the various models.

#### 4. Conclusion

In this study,  $\alpha$ -decay half-lives of some neutron-deficient nuclei within the range of  $80 \leq Z \leq 118$  have been calculated using Coulomb and proximity potential model (CPPM), temperature dependent Coulomb and proximity potential model (CPPMT), Royer formula, New RenB (NRB) formula, and a trained artificial neural network ( $T^{ANN}$ ) model. New coefficients were obtained for the Royer and NRB empirical formulas with the aid of a least square fit scheme and input data from NUBASE2020 database. When compared with the experimental data, all models are found to give very good predictions of the half-lives. The CPPMT was found to perform better than CPPM, indicating the importance of using temperature-dependent nuclear potentials. With a root mean square error of 0.3843, the  $T^{ANN}$  model is found to give the best performance in predicting the half-lives of the neutron-deficient nuclei. The second stage of the study was to predict the half-lives of  $\alpha$ -decay from unmeasured neutron-deficient nuclei. To achieve this, the  $Q_\alpha$  values were required as inputs. Following the success of the ANN in predicting the half-lives, we were motivated to train another ANN to predict  $Q_\alpha$  values (denoted as  $Q_\alpha^{ANN}$ ). When compared to experimental  $Q_\alpha$  values and theoretically predicted ones by WS4 and WS4+RBF formulas, the ANN model is found to give very good descriptions of the  $Q_\alpha$  values. The  $Q_\alpha^{ANN}$  values were then used as inputs to predict the half-lives of  $\alpha$ -decay from unmeasured neutron-deficient nuclei.

using CPPM, CPPMT, improved Royer formula, improved NRB formula and the  $T^{ANN}$  model. The results of the predicted half-lives by our models are found to be in good agreements with those predicted using generalized liquid drop model (GLDM). This study concludes that half-lives of  $\alpha$ -decay from neutron-deficient nuclei can successfully be predicted using ANN, and this can contribute to the determination of nuclei at the driplines.

## REFERENCES

- [1] K. P. Santhosh, Dashty T. Akrawy, H. Hassanabadi, Ali H. Ahmed, and Tinu Ann Jose.  $\alpha$ -decay half-lives of lead isotopes within a modified generalized liquid drop model. *Physical Review C*, 101:064610, 2020.
- [2] J H Cheng, J L Chen, J G Deng, X J Wu, X H Li, and P C Chu. Systematic study of  $\alpha$  decay half-lives based on gamow-like model with a screened electrostatic barrier. *Nuclear Physics A*, 987:350–368, 2019.
- [3] A. Zdeb, M. Warda, and K. Pomorski. Half-lives for  $\alpha$  and cluster radioactivity within a gamow-like model. *Physical Review C*, 87:024308, 2013.
- [4] G. Gamow. The quantum theory of nuclear disintegration. *Nature*, 122:805–806, 1928.
- [5] R. W. Gurney and E. U. Condon. Wave mechanics and radioactive disintegration. *Nature*, 122:439–439, 1928.
- [6] R. W. Gurney and E. U. Condon. Quantum mechanics and radioactive disintegration. *Physical Review*, 33:127–140, 1929.
- [7] O A P Tavares, S B Duarte, O Rodríguez, F Guzmán, M Gonçalves, and F García. Effective liquid drop description for alpha decay of atomic nuclei. *Journal of Physics G*, 24:1757–1775, 1998.
- [8] J.P. Cui, Y.H. Gao, Y.Z. Wang, and J.Z. Gu. Improved effective liquid drop model for  $\alpha$ -decay half-lives. *Nuclear Physics A*, 1017:122341, 2021.
- [9] G. Royer and B. Remaud. Static and dynamic fusion barriers in heavy-ion reactions. *Nuclear Physics A*, 444:477–497, 1985.
- [10] X. Bao, H. Zhang, H. Zhang, G. Royer, and J. Li. Systematical calculation of  $\alpha$  decay half-lives with a generalized liquid drop model. *Nuclear Physics A*, 921:85–95, 2014.
- [11] N. N. Ma, H. F. Zhang, J. M. Dong, and H. F. Zhang. *Alpha-decay half-life with a generalized liquid drop model by using a precise decay energy*, pages 105–108. 2016.
- [12] K. P. Santhosh and Tinu Ann Jose. Half-lives of cluster radioactivity using the modified generalized liquid drop model with a new preformation factor. *Physical Review C*, 99:064604, 2019.
- [13] D. T. Akrawy, K. P. Santhosh, and H. Hassanabadi.  $\alpha$ -decay half-lives of some superheavy nuclei within a modified generalized liquid drop model. *Physical Review C*, 100:034608, 2019.

- [14] R. K. Gupta and W. Greiner. Cluster radioactivity. *International Journal of Modern Physics E*, 03:335–433, 1994.
- [15] B. Singh, S. K. Patra, and R. K. Gupta. Cluster radioactive decay within the preformed cluster model using relativistic mean-field theory densities. *Physical Review C*, 82:014607, 2010.
- [16] Y. J. Wang, H. F. Zhang, W. Zuo, and J. Q. Li. Improvement of a fission-like model for nuclear  $\alpha$  decay. 27:062103, 2010.
- [17] W. A. Yahya and B. J. Falaye. Alpha decay study of thorium isotopes using double folding model with NN interactions derived from relativistic mean field theory. *Nuclear Physics A*, 1015:122311, 2021.
- [18] W. A. Yahya and K. J. Oyewunmi. Calculations of the alpha decay half-lives of some polonium isotopes using the double folding model. *Acta Physica Polonica B*, 52:1357–1372, 2021.
- [19] G Royer. Alpha emission and spontaneous fission through quasi-molecular shapes. *Journal of Physics G: Nuclear and Particle Physics*, 26:1149–1170, 2000.
- [20] G. Royer. Analytic expressions for alpha-decay half-lives and potential barriers. *Nuclear Physics A*, 848:279–291, 2010.
- [21] J. G. Deng, H. F. Zhang, and G. Royer. Improved empirical formula for  $\alpha$ -decay half-lives. *Physical Review C*, 101:034307, 2020.
- [22] V. Yu. Denisov and A. A. Khudenko. Erratum: $\alpha$ -decay half-lives: Empirical relations [phys. rev. *Physical Review C*, 82:054614, 2010].
- [23] V.E. Viola and G.T. Seaborg. Nuclear systematics of the heavy elements—II lifetimes for alpha, beta and spontaneous fission decay. *Journal of Inorganic and Nuclear Chemistry*, 28:741–761, 1966.
- [24] Z. Ren, C. Xu, and Z. Wang. New perspective on complex cluster radioactivity of heavy nuclei. *Physical Review C*, 70:034304, 2004.
- [25] D. T. Akrawy, H. Hassanabadi, Y. Qian, and K.P. Santhosh. Influence of nuclear isospin and angular momentum on  $\alpha$ -decay half-lives. *Nuclear Physics A*, 983:310–320, 2018.
- [26] C. Qi, F. R. Xu, R. J. Liotta, R. Wyss, M. Y. Zhang, C. Asawatangtrakuldee, and D. Hu. Microscopic mechanism of charged-particle radioactivity and generalization of the geiger-nuttall law. *Physical Review C*, 80:044326, 2009.
- [27] D T Akrawy and D N Poenaru. Alpha decay calculations with a new formula. *Journal of Physics G: Nuclear and Particle Physics*, 44:105105, 2017.
- [28] Y. Z. Wang, J. P. Cui, Y. L. Zhang, S. Zhang, and J. Z. Gu. Competition between  $\alpha$  decay and proton radioactivity of neutron-deficient nuclei. *Physical Review C*, 95:014302, 2017.
- [29] J.P. Cui, Y. Xiao, Y.H. Gao, and Y.Z. Wang.  $\alpha$ -decay half-lives of neutron-deficient nuclei. *Nuclear Physics A*, 987:99–111, 2019.
- [30] C. Qi. Alpha decay as a probe for the structure of neutron-deficient nuclei. *Reviews in Physics*, 1:77–89, 2016.
- [31] Y. Gao, J. Cui, Y. Wang, and J. Gu. Cluster radioactivity of neutron-deficient nuclei in trans-tin region. *Scientific Reports*, 10:9119, 2020.

- [32] A. Adel and A. R. Abdulghany. Proton radioactivity and  $\alpha$ -decay of neutron-deficient nuclei. *Physica Scripta*, 96:125314, 2021.
- [33] H.C. Manjunatha. Alpha decay properties of superheavy nuclei  $z = 126$ . *Nuclear Physics A*, 945:42–57, 2015.
- [34] W.A. Yahya. Alpha decay half-lives of  $^{171-189}\text{Hg}$  isotopes using modified gamow-like model and temperature dependent proximity potential. *Journal of the Nigerian Society of Physical Sciences*, 2:250–256, 2020.
- [35] V. Zanganah, Dashty T. Akrawy, H. Hassanabadi, S.S. Hosseini, and Shagun Thakur. Calculation of  $\alpha$ -decay and cluster half-lives for 197–226fr using temperature-dependent proximity potential model. *Nuclear Physics A*, 997:121714, 2020.
- [36] K.P. Santhosh, B. Priyanka, and M.S. Unnikrishnan. Cluster decay half-lives of trans-lead nuclei within the coulomb and proximity potential model. *Nuclear Physics A*, 889:29–50, 2012.
- [37] L. Vanneschi and M. Castelli. Multilayer perceptrons. In *Encyclopedia of Bioinformatics and Computational Biology*, volume 1-3, pages 612–620. Elsevier, 2019.
- [38] S Akkoyun, T Bayram, S O Kara, and A Sinan. An artificial neural network application on nuclear charge radii. *Journal of Physics G: Nuclear and Particle Physics*, 40:055106, 2013.
- [39] Di Wu, C. L. Bai, H. Sagawa, and H. Q. Zhang. Calculation of nuclear charge radii with a trained feed-forward neural network. *Physical Review C*, 102:054323, 2020.
- [40] Z. M. Niu, H. Z. Liang, B. H. Sun, W. H. Long, and Y. F. Niu. Predictions of nuclear  $\beta$ -decay half-lives with machine learning and their impact on r-process nucleosynthesis. *Physical Review C*, 99:064307, 2019.
- [41] V. Jetly and B. Chaudhury. Extracting electron scattering cross sections from swarm data using deep neural networks. *Machine Learning: Science and Technology*, 2:035025, 2021.
- [42] S. Akkoyun and T. Bayram. Shell model calculations for proton-rich zn isotopes via new generated effective interaction by artificial neural networks. *Cumhuriyet Science Journal*, 40:570–577, 2019.
- [43] U. Baños Rodríguez, C. Zuñiga Vargas, M. Gonçalves, S. B. Duarte, and F. Guzmán. Alpha half-lives calculation of superheavy nuclei with q  $\alpha$ -value predictions based on the bayesian neural network approach. *Journal of Physics G: Nuclear and Particle Physics*, 46:115109, 2019.
- [44] F.G. Kondev, M. Wang, W.J. Huang, S. Naimi, and G. Audi. The nubase2020 evaluation of nuclear physics properties. *Chinese Physics C*, 45:030001, 2021.
- [45] L. Wang, Z. Zhang, X. Zhang, X. Zhou, P. Wang, and Y. Zheng. A deep-forest based approach for detecting fraudulent online transaction. In *Advances in Computers*, volume 120, pages 1–38. Elsevier, 2021.
- [46] N. Wang, M. Liu, X. Wu, and J. Meng. Surface diffuseness correction in global mass formula. *Physics Letters B*, 734:215–219, 2014.

- [47] Y.-J. Shi and W.J. Swiatecki. Estimates of the influence of nuclear deformations and shell effects on the lifetimes of exotic radioactivities. *Nuclear Physics A*, 464:205–222, 1987.
- [48] S. S. Malik and R. K. Gupta. Theory of cluster radioactive decay and of cluster formation in nuclei. *Physical Review C*, 39:1992–2000, 1989.
- [49] J. Blocki, J. Randrup, W.J. Swiatecki, and C.F. Tsang. Proximity forces. *Annals of Physics*, 105:427–462, 1977.
- [50] R. Gharaei and V. Zanganeh. Temperature-dependent potential in cluster-decay process. *Nuclear Physics A*, 952:28–40, 2016.
- [51] S. A. Gurvitz and G. Kalbermann. Decay width and the shift of a quasistationary state. *Physical Review Letters*, 59:262–265, 1987.
- [52] M. Salehi and O. N. Ghodsi. The influence of the dependence of surface energy coefficient to temperature in the proximity model. *Chinese Physics Letters*, 30:042502, 2013.
- [53] G. Sauer, H. Chandra, and U. Mosel. Thermal properties of nuclei. *Nuclear Physics A*, 264:221–243, 1976.
- [54] S. Shlomo and J. B. Natowitz. Temperature and mass dependence of level density parameter. *Physical Review C*, 44:2878–2880, 1991.
- [55] R K Gupta, S Singh, R K Puri, A Sandulescu, W Greiner, and W Scheid. Influence of the nuclear surface diffuseness on exotic cluster decay half-life times. *Journal of Physics G: Nuclear and Particle Physics*, 18:1533–1542, 1992.
- [56] R K Puri and R K Gupta. Alpha-cluster transfer process in colliding s-d shell nuclei using the energy density formalism. *Journal of Physics G: Nuclear and Particle Physics*, 18:903–915, 1992.
- [57] D. Ni, Z. Ren, T. Dong, and C. Xu. Unified formula of half-lives for  $\alpha$  decay and cluster radioactivity. *Physical Review C*, 78:044310, 2008.